



Vibration analysis of porous metal foam plates rested on viscoelastic substrate

Farzad Ebrahimi¹ · Ali Dabbagh² · Mehdi Taheri²

Received: 12 December 2019 / Accepted: 23 April 2020 / Published online: 12 May 2020
© Springer-Verlag London Ltd., part of Springer Nature 2020

Abstract

In this paper, the vibration problem of a rectangular plate rested on a viscoelastic substrate and consisting of porous metal foam is solved via an analytical method with respect to the influences of various porosity distributions. Three types of porosity distribution across the thickness are covered, namely uniform, symmetric and asymmetric. The strain–displacement relations of the plate are assumed to be derived on the basis of a refined higher-order shear deformation plate theory. Then, the achieved relations will be incorporated with the Hamilton’s principle in order to reach the Euler–Lagrange equations of the structure. Next, the well-known Galerkin’s method is utilized to calculate the natural frequencies of the system. The influences of both simply supported and clamped boundary conditions are included. In order to show the accuracy of the presented method, the results of present research are compared with those reported by former published papers. The reported results show that an increase in the porosity coefficient can dramatically decrease the frequency of the plate. Also, the stiffness of the system can be lesser decreased, while a symmetrically porous metal foam is used to manufacture the plate.

Keywords Vibration analysis · Metal foam · Uniform and non-uniform porosity distributions · Viscoelastic medium · Galerkin’s method

1 Introduction

Porosity is a defect which is able to affect the mechanical performance of a system. Usually, porosity leads to a softening influence on the stiffness of a continuous system made from porous materials. Henceforward, the system’s frequency or stability limit decreases gradually as the porosity coefficient grows. Due to the unavoidable presence of porosity in the fabricated materials, this phenomenon has recently attracted the researchers’ attention. For instance, Jabbari et al. [1] analyzed the stability responses of porous functionally graded (FG) circular plates. Another porosity-dependent paper is presented by

Jabbari et al. [2] in order to consider the stability behaviors of circular FG plates, while the structure is subjected to thermal loading. Also, Wattanasakulpong and Ungbhakorn [3] investigated the vibrational behaviors of porous FG beams once the ends of the structure were considered to be restrained. Later, Chen et al. [4] investigated the static stability of porous FG beams via a theory which is able to capture the effects of shear deformation. Moreover, both natural and externally excited dynamic behaviors of FG beams are probed by Chen et al. [5] with respect to the influences of porosity. In another study, a porous FG core is considered by Chen et al. [6] to survey the nonlinear dynamic responses of multilayered beams. Rezaei and Saidi [7] studied the vibrational characteristics of porous rectangular plates within the frameworks of the Carrera’s unified formulation (CUF). Atmane et al. [8] studied the dynamic frequency and deflection behaviors of porous FG beams via a shear deformable beam model. Recently, Barati and Zenkour [9] have probed the thermo-electrically influenced vibrational behaviors of porous FG plates

✉ Farzad Ebrahimi
febrahimi@eng.ikiu.ac.ir

¹ Department of Mechanical Engineering, Faculty of Engineering, Imam Khomeini International University, Qazvin, Iran

² School of Mechanical Engineering, College of Engineering, University of Tehran, Tehran, Iran

considering for the effects of various supports at the edges of the structure.

As discussed in the above sentences, the influences of porosity on the mechanical behaviors of FG structures have been widely studied by a large number of researchers. However, the issue of static and dynamic behaviors of porous metal foam beams, plates and shells has lesser been studied by the scientific community. Although this issue has not been investigated a lot, many natural materials such as wood, bone and cork can be well simulated by making porous metal foams [10]. Also, metal foams are excellent candidates for the conditions which both high stiffness and low density are required together. So, it is of great importance to earn as more as possible knowledge about the mechanical behaviors of beams, plates and shells made from metal foams.

In one of the researches in this field, Vaidya et al. [11] investigated both low and immediate velocity impact responses of sandwich plates including a metal foam core. The issue of dynamic buckling characteristics of metal foam plates is probed by Debowski et al. [12] in the framework of Bubnov–Galerkin method. Magnucka-Blandzi [13] investigated the critical stability responses of laminated plates with a porous metal foam core in a bi-axial compression. The plastic behaviors of a laminate beam with metal foam core are observed by Qin and Wang [14] focusing on the variations of the force versus the transverse deflection of the structure once a punch is touching the beam. In addition, Jasion et al. [15] procured a local stability analysis on the behaviors of laminated beams and plates made from a central metal foam layer coated with facesheets by considering the wrinkling effects. Qin et al. [16] surveyed the impact responses of sandwich plates that consisted of a metal foam core via both analytical and finite element methods. Toan Thang et al. [10] could solve the postbuckling problem of porous metal foam cylinders with respect to various porosity distributions across the shell's thickness. They derived the strain–displacement relations by combining the classical shell theory with the nonlinear theory of von-Karman. Most recently, a porosity-dependent homogenization scheme has been utilized by Ebrahimi et al. [17] in order to probe the free oscillation problem of cylinders manufactured from porous metal foams.

According to the above literature review, it can be comprehended that there exists no analytical investigation on the viscoelastically damped dynamic problem of rectangular plates that consisted of porous metal foams up to now. Therefore, the authors are aimed to solve the aforementioned problem by the means of an analytical approach. The plate will be modeled based on the refined shear deformation theory of plates incorporated with the dynamic form of the principle of virtual work. Among

three types of porosity distributions, symmetric one provides higher natural frequencies followed by asymmetric and uniform types.

2 Theory and formulations

2.1 Derivation of the effective properties of porous metal foams

In this section, the influences of three types of porosity on the effective material properties of porous metal foam shells will be shown. The schematic representation of the porosity through the thickness of the shell can be seen in Fig. 1. In the following formulations e_0 and e_m denote the porosity coefficient and density coefficients, respectively. The effective properties for a uniformly porous metal foam can be written as [17]:

$$E(z) = E_1(1 - e_0\lambda) \quad (1)$$

$$G(z) = G_1(1 - e_0\lambda) \quad (2)$$

$$\rho(z) = \rho_1\sqrt{1 - e_0\lambda} \quad (3)$$

Equations (1)–(3) can be rewritten for the symmetric porosity distribution as [17]:

$$E(z) = E_1\left(1 - e_0\cos\left(\frac{\pi z}{h}\right)\right) \quad (4)$$

$$G(z) = G_1\left(1 - e_0\cos\left(\frac{\pi z}{h}\right)\right) \quad (5)$$

$$\rho(z) = \rho_1\left(1 - e_m\cos\left(\frac{\pi z}{h}\right)\right) \quad (6)$$

And for the asymmetric porosity distribution, one should calculate the effective material properties as follows [17]:

$$E(z) = E_1\left(1 - e_0\cos\left(\frac{\pi z}{2h} + \frac{\pi}{4}\right)\right) \quad (7)$$

$$G(z) = G_1\left(1 - e_0\cos\left(\frac{\pi z}{2h} + \frac{\pi}{4}\right)\right) \quad (8)$$

$$\rho(z) = \rho_1\left(1 - e_m\cos\left(\frac{\pi z}{2h} + \frac{\pi}{4}\right)\right) \quad (9)$$

in which E_1 , G_1 and ρ_1 are the maximum values of Young's modulus, shear modulus and mass density of the porous metal foam, respectively. Also, E_2 , G_2 and ρ_2 are the minimum values of the aforementioned variants, respectively. Based on the extremum values, the porosity and density coefficients can be defined in the following form [17]:

$$e_0 = 1 - \frac{E_2}{E_1} = 1 - \frac{G_2}{G_1}, \quad (0 < e_0 < 1) \quad (10)$$

$$e_m = 1 - \frac{\rho_2}{\rho_1} \quad (11)$$

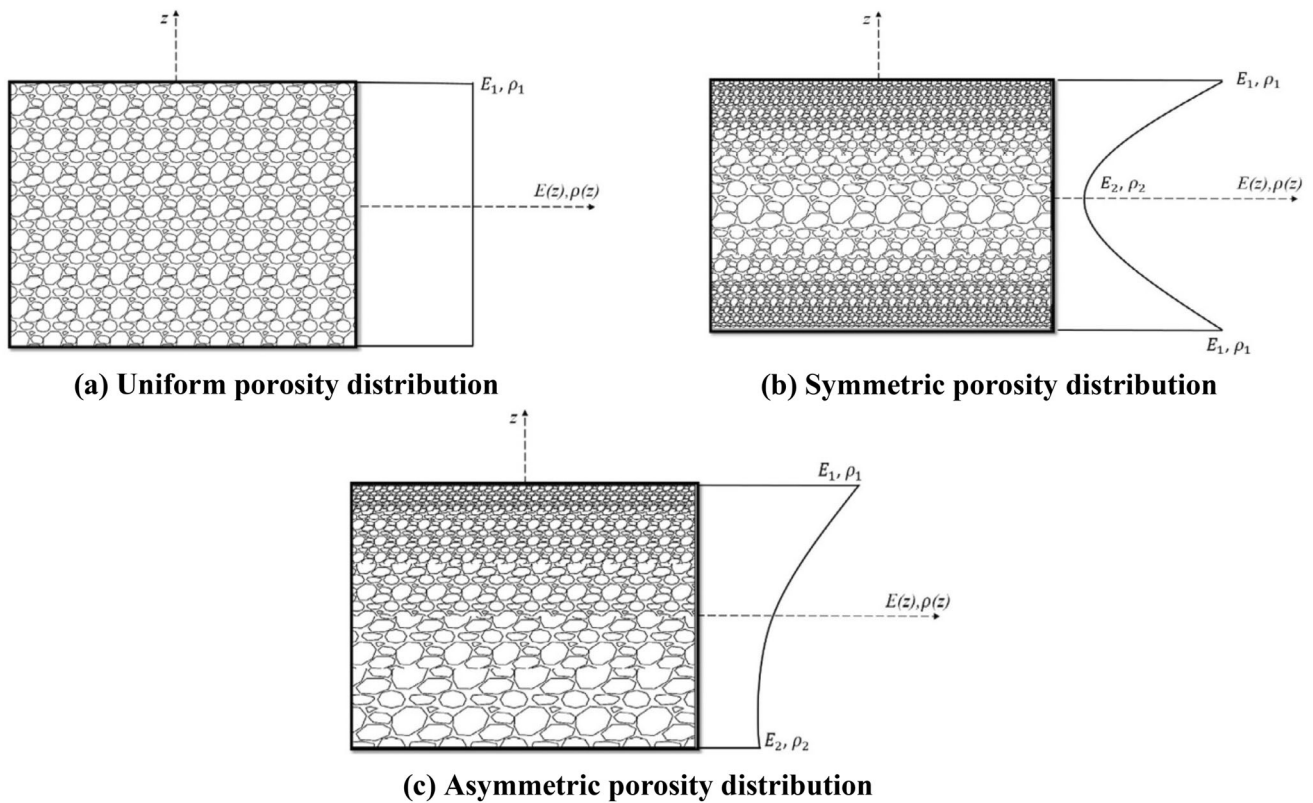


Fig. 1 Schematic illustration of various porosity distributions across the plate’s thickness for **a** uniform porosity distribution, **b** symmetric porosity distribution and **c** asymmetric porosity distribution

In this method, the variations of the Poisson’s ratio are small enough to be considered negligible. So, the Poisson’s is constant. Moreover, the term λ which is implemented in Eqs. (1)–(3) can be calculated by [17]:

$$\lambda = \frac{1}{e_0} - \frac{1}{e_0} \left[\frac{2}{\pi} \sqrt{1 - e_0} - \frac{2}{\pi} + 1 \right]^2 \tag{12}$$

2.2 Kinematic relations

The kinematic relations of the plate are going to be derived in this section. The displacement fields of a rectangular plate can be expressed as follows based on the refined higher-order shear deformable plate theory [18–20]:

$$\begin{aligned} u_x(x, y, z, t) &= u(x, y, t) - z \frac{\partial w_b(x, y, t)}{\partial x} - f(z) \frac{\partial w_s(x, y, t)}{\partial x}, \\ u_y(x, y, z, t) &= v(x, y, t) - z \frac{\partial w_b(x, y, t)}{\partial y} - f(z) \frac{\partial w_s(x, y, t)}{\partial y}, \\ u_z(x, y, z, t) &= w_b(x, y, t) + w_s(x, y, t). \end{aligned} \tag{13}$$

In the above equations, u and v are longitudinal and transverse displacements of the mid-surface, respectively; also, w_b and w_s are the bending and shear deflections through z -axis, respectively. In addition, $f(z)$ stands for the

shape function of the theorem. Now, the nonzero strains of the plate can be expressed by following equations [18–20]:

$$\begin{aligned} \begin{Bmatrix} \varepsilon_{xx} \\ \varepsilon_{yy} \\ \gamma_{xy} \end{Bmatrix} &= \begin{Bmatrix} \varepsilon_{xx}^0 \\ \varepsilon_{yy}^0 \\ \gamma_{xy}^0 \end{Bmatrix} + z \begin{Bmatrix} \kappa_{xx}^b \\ \kappa_{yy}^b \\ \kappa_{xy}^b \end{Bmatrix} + f(z) \begin{Bmatrix} \kappa_{xx}^s \\ \kappa_{yy}^s \\ \kappa_{xy}^s \end{Bmatrix}, \\ \begin{Bmatrix} \gamma_{xz} \\ \gamma_{yz} \end{Bmatrix} &= g(z) \begin{Bmatrix} \gamma_{xz}^0 \\ \gamma_{yz}^0 \end{Bmatrix} \end{aligned} \tag{14}$$

where

$$\begin{aligned} \begin{Bmatrix} \varepsilon_{xx}^0 \\ \varepsilon_{yy}^0 \\ \gamma_{xy}^0 \end{Bmatrix} &= \begin{Bmatrix} \frac{\partial u}{\partial x} \\ \frac{\partial v}{\partial y} \\ \frac{\partial u}{\partial y} + \frac{\partial v}{\partial x} \end{Bmatrix}, \quad \begin{Bmatrix} \kappa_{xx}^b \\ \kappa_{yy}^b \\ \kappa_{xy}^b \end{Bmatrix} = \begin{Bmatrix} -\frac{\partial^2 w_b}{\partial x^2} \\ -\frac{\partial^2 w_b}{\partial y^2} \\ -2\frac{\partial^2 w_b}{\partial x \partial y} \end{Bmatrix}, \\ \begin{Bmatrix} \kappa_{xx}^s \\ \kappa_{yy}^s \\ \kappa_{xy}^s \end{Bmatrix} &= \begin{Bmatrix} -\frac{\partial^2 w_s}{\partial x^2} \\ -\frac{\partial^2 w_s}{\partial y^2} \\ -2\frac{\partial^2 w_s}{\partial x \partial y} \end{Bmatrix}, \quad \begin{Bmatrix} \gamma_{xz}^0 \\ \gamma_{yz}^0 \end{Bmatrix} = \begin{Bmatrix} \frac{\partial w_s}{\partial x} \\ \frac{\partial w_s}{\partial y} \end{Bmatrix} \end{aligned} \tag{15}$$

In this research, the following novel shape function is utilized [21]:

$$f(z) = \frac{hc^z}{h^2 + \pi^2} \left(\pi \sin\left(\frac{\pi z}{h}\right) + h \cos\left(\frac{\pi z}{h}\right) \right) - \frac{h^2}{h^2 + \pi^2} \quad (16)$$

2.3 Derivation of motion equations

Herein, dynamic form of the principle of virtual work will be extended for plates in order to reach the Euler–Lagrange equations of a porous metal foam plate. This principle can be defined in the following form [19, 20]:

$$\int_0^t \delta(U - K - V) dt = 0 \quad (17)$$

where U , K and V are strain energy, kinetic energy and work done by external loading, respectively. The variation of strain energy for a linear elastic solid can be expressed as [19, 20]:

$$\delta U = \int_V (\sigma_{xx} \delta \varepsilon_{xx} + \sigma_{yy} \delta \varepsilon_{yy} + \sigma_{xy} \delta \gamma_{xy} + \sigma_{xz} \delta \gamma_{xz} + \sigma_{yz} \delta \gamma_{yz}) dV$$

$$= \int_0^b \int_0^a \left(N_{xx} \delta \varepsilon_{xx}^0 + M_{xx}^b \delta \kappa_{xx}^b + M_{xx}^s \delta \kappa_{xx}^s + N_{yy} \delta \varepsilon_{yy}^0 + M_{yy}^b \delta \kappa_{yy}^b + M_{yy}^s \delta \kappa_{yy}^s + N_{xy} \delta \gamma_{xy}^0 + M_{xy}^b \delta \kappa_{xy}^b + M_{xy}^s \delta \kappa_{xy}^s + Q_{xz} \delta \gamma_{xz}^0 + Q_{yz} \delta \gamma_{yz}^0 \right) dx dy \quad (18)$$

in the above equation, the axial forces and bending and shear moments can be defined as:

$$(N_{ij}, M_{ij}^b, M_{ij}^s) = \int_{-h/2}^{h/2} (1, z, f(z)) \sigma_{ij} dz, \quad (i, j = x, y),$$

$$Q_k = \int_{-h/2}^{h/2} g(z) \sigma_k dz, \quad (k = xz, yz) \quad (19)$$

where $g(z) = 1 - df(z)/dz$. The first variation of kinetic energy can be expressed as [19, 20]:

$$\delta K = \int_V (\dot{u}_x \delta \dot{u}_x + \dot{u}_y \delta \dot{u}_y + \dot{u}_z \delta \dot{u}_z) \rho(z) dV$$

$$= \int_0^b \int_0^a \left(I_0 \left(\frac{\partial u}{\partial t} \frac{\partial \delta u}{\partial t} + \frac{\partial v}{\partial t} \frac{\partial \delta v}{\partial t} + \frac{\partial w}{\partial t} \frac{\partial \delta w}{\partial t} \right) - I_1 \left(\frac{\partial u}{\partial t} \frac{\partial^2 \delta w_b}{\partial x \partial t} + \frac{\partial^2 w_b}{\partial x \partial t} \frac{\partial \delta u}{\partial t} + \frac{\partial v}{\partial t} \frac{\partial^2 \delta w_b}{\partial y \partial t} + \frac{\partial^2 w_b}{\partial y \partial t} \frac{\partial \delta v}{\partial t} \right) - J_1 \left(\frac{\partial u}{\partial t} \frac{\partial^2 \delta w_s}{\partial x \partial t} + \frac{\partial^2 w_s}{\partial x \partial t} \frac{\partial \delta u}{\partial t} + \frac{\partial v}{\partial t} \frac{\partial^2 \delta w_s}{\partial y \partial t} + \frac{\partial^2 w_s}{\partial y \partial t} \frac{\partial \delta v}{\partial t} \right) + I_2 \left(\frac{\partial^2 w_b}{\partial x \partial t} \frac{\partial^2 \delta w_b}{\partial x \partial t} + \frac{\partial^2 w_b}{\partial y \partial t} \frac{\partial^2 \delta w_b}{\partial y \partial t} \right) + K_2 \left(\frac{\partial^2 w_s}{\partial x \partial t} \frac{\partial^2 \delta w_s}{\partial x \partial t} + \frac{\partial^2 w_s}{\partial y \partial t} \frac{\partial^2 \delta w_s}{\partial y \partial t} \right) + J_2 \left(\frac{\partial^2 w_b}{\partial x \partial t} \frac{\partial^2 \delta w_s}{\partial x \partial t} + \frac{\partial^2 w_s}{\partial x \partial t} \frac{\partial^2 \delta w_b}{\partial x \partial t} + \frac{\partial^2 w_b}{\partial y \partial t} \frac{\partial^2 \delta w_s}{\partial y \partial t} + \frac{\partial^2 w_s}{\partial y \partial t} \frac{\partial^2 \delta w_b}{\partial y \partial t} \right) \right) dx dy \quad (20)$$

In all of the equations, the dot-superscript denotes the differentiation with respect to time, and the mass inertias used in the above equations are given in the following form:

$$[I_0, I_1, J_1, I_2, J_2, K_2] = \int_{-h/2}^{h/2} [1, z, f(z), z^2, zf(z), f^2(z)] \rho(z) dz \quad (21)$$

Furthermore, the variation of work done by external loading can be stated in the following form [20]:

$$\delta V = \int_A \left[N_x^0 \frac{\partial(w_b+w_s)}{\partial x} \frac{\partial \delta(w_b+w_s)}{\partial x} + N_y^0 \frac{\partial(w_b+w_s)}{\partial y} \frac{\partial \delta(w_b+w_s)}{\partial y} + 2 \delta N_{xy}^0 \frac{\partial(w_b+w_s)}{\partial x} \frac{\partial \delta(w_b+w_s)}{\partial y} - k_w (w_b + w_s) \delta (w_b + w_s) + k_p \left(\frac{\partial^2 (w_b + w_s)}{\partial x^2} + \frac{\partial^2 (w_b + w_s)}{\partial y^2} \right) \delta (w_b + w_s) - c_d \frac{\partial (w_b + w_s)}{\partial t} \delta (w_b + w_s) \right] dA \quad (22)$$

in which N_x^0 , N_y^0 and N_{xy}^0 are external in-plane loads that are applied to the structure. Also, k_w and k_p are the elastic linear and shear stiffnesses of substrate, respectively, and c_d denotes the damping coefficient of the substrate.

By substituting Eqs. (18), (20) and (22) into Eq. (17) and setting the coefficients of δu , δv , δw_b and δw_s to zero, the Euler–Lagrange equations of porous metal foam plates can be written as [18–20]:

$$\frac{\partial N_{xx}}{\partial x} + \frac{\partial N_{xy}}{\partial y} = I_0 \frac{\partial^2 u}{\partial t^2} - I_1 \frac{\partial^3 w_b}{\partial x \partial t^2} - J_1 \frac{\partial^3 w_s}{\partial x \partial t^2} \quad (23)$$

$$\frac{\partial N_{xy}}{\partial x} + \frac{\partial N_{yy}}{\partial y} = I_0 \frac{\partial^2 v}{\partial t^2} - I_1 \frac{\partial^3 w_b}{\partial y \partial t^2} - J_1 \frac{\partial^3 w_s}{\partial y \partial t^2} \quad (24)$$

$$\frac{\partial^2 M_{xx}^b}{\partial x^2} + 2 \frac{\partial^2 M_{xy}^b}{\partial x \partial y} + \frac{\partial^2 M_{yy}^b}{\partial y^2} - k_w (w_b + w_s) + k_p \left(\frac{\partial^2 (w_b + w_s)}{\partial x^2} + \frac{\partial^2 (w_b + w_s)}{\partial y^2} \right) - c_d \frac{\partial (w_b + w_s)}{\partial t} = I_0 \frac{\partial^2 (w_b + w_s)}{\partial t^2} + I_1 \left(\frac{\partial^3 u}{\partial x \partial t^2} + \frac{\partial^3 v}{\partial y \partial t^2} \right) - I_2 \left(\frac{\partial^4 w_b}{\partial x^2 \partial t^2} + \frac{\partial^4 w_b}{\partial y^2 \partial t^2} \right) - J_2 \left(\frac{\partial^4 w_s}{\partial x^2 \partial t^2} + \frac{\partial^4 w_s}{\partial y^2 \partial t^2} \right) \quad (25)$$

$$\frac{\partial^2 M_{xx}^s}{\partial x^2} + 2 \frac{\partial^2 M_{xy}^s}{\partial x \partial y} + \frac{\partial^2 M_{yy}^s}{\partial y^2} + \frac{\partial Q_{xz}}{\partial x} + \frac{\partial Q_{yz}}{\partial y} - k_w (w_b + w_s) + k_p \left(\frac{\partial^2 (w_b + w_s)}{\partial x^2} + \frac{\partial^2 (w_b + w_s)}{\partial y^2} \right) - c_d \frac{\partial (w_b + w_s)}{\partial t} = I_0 \frac{\partial^2 (w_b + w_s)}{\partial t^2} + J_1 \left(\frac{\partial^3 u}{\partial x \partial t^2} + \frac{\partial^3 v}{\partial y \partial t^2} \right) - J_2 \left(\frac{\partial^4 w_b}{\partial x^2 \partial t^2} + \frac{\partial^4 w_b}{\partial y^2 \partial t^2} \right) - K_2 \left(\frac{\partial^4 w_s}{\partial x^2 \partial t^2} + \frac{\partial^4 w_s}{\partial y^2 \partial t^2} \right) \quad (26)$$

2.4 Constitutive equations

Herein, the elastic stress–strain relations of isotropic composite materials are reviewed for the purpose of deriving the fundamental elastic equations of such solids. Here, the following constitutive equations can be expressed as [22]:

$$\sigma_{ij} = C_{ijkl}\epsilon_{kl} \tag{27}$$

where σ_{ij} , ϵ_{kl} and C_{ijkl} represent the components of Cauchy stress tensor, strain tensor and elasticity tensor, respectively. Therefore, these relations can be modified as follows for plates [22]:

$$\begin{bmatrix} \sigma_{xx} \\ \sigma_{yy} \\ \sigma_{yz} \\ \sigma_{xz} \\ \sigma_{xy} \end{bmatrix} = \begin{bmatrix} Q_{11} & Q_{12} & 0 & 0 & 0 \\ Q_{12} & Q_{22} & 0 & 0 & 0 \\ 0 & 0 & Q_{44} & 0 & 0 \\ 0 & 0 & 0 & Q_{55} & 0 \\ 0 & 0 & 0 & 0 & Q_{66} \end{bmatrix} \begin{bmatrix} \epsilon_{xx} \\ \epsilon_{yy} \\ \epsilon_{yz} \\ \epsilon_{xz} \\ \epsilon_{xy} \end{bmatrix} \tag{28}$$

where

$$\begin{aligned} Q_{11} &= \frac{E}{1-\nu^2}, & Q_{12} &= \nu Q_{11}, & Q_{22} &= Q_{11}, \\ Q_{44} &= Q_{55} = Q_{66} = G \end{aligned} \tag{29}$$

By considering the porous metal foam as a linear elastic isotropic solid and integrating over the structure’s thickness, the force and moments of the plate can be expressed

in terms of the strains in the following form [19]:

in which

$$\begin{aligned} [A_n, B_n, B_n^s, D_n, D_n^s, H_n^s] &= \int_{-h/2}^{h/2} [1, z, f(z), z^2, zf(z), f^2(z)] Q_n(z) dz, \quad n = (11, 12, 22, 66) \\ [A_{44}^s, A_{55}^s] &= \int_{-h/2}^{h/2} [Q_{44}(z), Q_{55}(z)] g^2(z) dz \end{aligned} \tag{31}$$

2.5 Governing equations

The coupled partial differential governing equations of a porous metal foam plate can be formulated in the following form by inserting Eq. (30) in Eqs. (23)–(26) [19]:

$$\begin{aligned} A_{11} \frac{\partial^2 u}{\partial x^2} + A_{66} \frac{\partial^2 u}{\partial y^2} + (A_{12} + A_{66}) \frac{\partial^2 v}{\partial x \partial y} - B_{11} \frac{\partial^3 w_b}{\partial x^3} \\ - (B_{12} + 2B_{66}) \frac{\partial^3 w_b}{\partial x \partial y^2} \\ - B_{11}^s \frac{\partial^3 w_s}{\partial x^3} - (B_{12}^s + 2B_{66}^s) \frac{\partial^3 w_s}{\partial x \partial y^2} - I_0 \frac{\partial^2 u}{\partial t^2} \\ + I_1 \frac{\partial^3 w_b}{\partial x \partial t^2} + J_1 \frac{\partial^3 w_b}{\partial x \partial t^2} = 0 \end{aligned} \tag{32}$$

$$\begin{bmatrix} N_{xx} \\ N_{yy} \\ N_{xy} \\ M_{xx}^b \\ M_{yy}^b \\ M_{xy}^b \\ M_{xx}^s \\ M_{yy}^s \\ M_{xy}^s \end{bmatrix} = \begin{bmatrix} A_{11} & A_{12} & 0 & B_{11} & B_{12} & 0 & B_{11}^s & B_{12}^s & 0 \\ A_{12} & A_{22} & 0 & B_{12} & B_{22} & 0 & B_{12}^s & B_{22}^s & 0 \\ 0 & 0 & A_{66} & 0 & 0 & B_{66} & 0 & 0 & B_{66}^s \\ B_{11} & B_{12} & 0 & D_{11} & D_{12} & 0 & D_{11}^s & D_{12}^s & 0 \\ B_{12} & B_{22} & 0 & D_{12} & D_{22} & 0 & D_{12}^s & D_{22}^s & 0 \\ 0 & 0 & B_{66} & 0 & 0 & D_{66} & 0 & 0 & D_{66}^s \\ B_{11}^s & B_{12}^s & 0 & D_{11}^s & D_{12}^s & 0 & H_{11}^s & H_{12}^s & 0 \\ B_{12}^s & B_{22}^s & 0 & D_{12}^s & D_{22}^s & 0 & H_{12}^s & H_{22}^s & 0 \\ 0 & 0 & B_{66}^s & 0 & 0 & D_{66}^s & 0 & 0 & H_{66}^s \end{bmatrix} \begin{bmatrix} \frac{\partial u}{\partial x} \\ \frac{\partial v}{\partial y} \\ \frac{\partial u}{\partial y} + \frac{\partial v}{\partial x} \\ -\frac{\partial^2 w_b}{\partial x^2} \\ -\frac{\partial^2 w_b}{\partial y^2} \\ -2\frac{\partial^2 w_b}{\partial x \partial y} \\ -\frac{\partial^2 w_s}{\partial x^2} \\ -\frac{\partial^2 w_s}{\partial y^2} \\ -2\frac{\partial^2 w_s}{\partial x \partial y} \end{bmatrix}, \quad \begin{bmatrix} Q_{xz} \\ Q_{yz} \end{bmatrix} = \begin{bmatrix} A_{44}^s & 0 \\ 0 & A_{55}^s \end{bmatrix} \begin{bmatrix} \frac{\partial w_s}{\partial x} \\ \frac{\partial w_s}{\partial y} \end{bmatrix} \tag{30}$$

$$\begin{aligned}
& (A_{12} + A_{66}) \frac{\partial^2 u}{\partial x \partial y} + A_{66} \frac{\partial^2 v}{\partial x^2} + A_{22} \frac{\partial^2 v}{\partial y^2} \\
& - (B_{12} + 2B_{66}) \frac{\partial^3 w_b}{\partial x^2 \partial y} - B_{22} \frac{\partial^3 w_b}{\partial y^3} \\
& - (B_{12}^s + 2B_{66}^s) \frac{\partial^3 w_s}{\partial x^2 \partial y} - B_{22}^s \frac{\partial^3 w_s}{\partial y^3} \\
& - I_0 \frac{\partial^2 v}{\partial t^2} + I_1 \frac{\partial^3 w_b}{\partial y \partial t^2} + J_1 \frac{\partial^3 w_b}{\partial y \partial t^2} = 0
\end{aligned} \tag{33}$$

$$\begin{aligned}
& B_{11} \frac{\partial^3 u}{\partial x^3} + (B_{12} + 2B_{66}) \left(\frac{\partial^3 u}{\partial x \partial y^2} + \frac{\partial^3 v}{\partial x^2 \partial y} \right) + B_{22} \frac{\partial^3 v}{\partial y^3} - \\
& D_{11} \frac{\partial^4 w_b}{\partial x^4} - 2(D_{12} + 2D_{66}) \frac{\partial^4 w_b}{\partial x^2 \partial y^2} - D_{22} \frac{\partial^4 w_b}{\partial y^4} \\
& - D_{11}^s \frac{\partial^4 w_s}{\partial x^4} - 2(D_{12}^s + 2D_{66}^s) \frac{\partial^4 w_s}{\partial x^2 \partial y^2} - D_{22}^s \frac{\partial^4 w_s}{\partial y^4} \\
& - k_w (w_b + w_s) + k_p \left(\frac{\partial^2 (w_b + w_s)}{\partial x^2} + \frac{\partial^2 (w_b + w_s)}{\partial y^2} \right) - c_d \frac{\partial (w_b + w_s)}{\partial t} \\
& - I_0 \frac{\partial^2 (w_b + w_s)}{\partial t^2} - I_1 \left(\frac{\partial^3 u}{\partial x \partial t^2} + \frac{\partial^3 v}{\partial y \partial t^2} \right) \\
& + I_2 \left(\frac{\partial^4 w_b}{\partial x^2 \partial t^2} + \frac{\partial^4 w_b}{\partial y^2 \partial t^2} \right) + J_2 \left(\frac{\partial^4 w_s}{\partial x^2 \partial t^2} + \frac{\partial^4 w_s}{\partial y^2 \partial t^2} \right) = 0
\end{aligned} \tag{34}$$

$$\begin{aligned}
& B_{11}^s \frac{\partial^3 u}{\partial x^3} + (B_{12}^s + 2B_{66}^s) \left(\frac{\partial^3 u}{\partial x \partial y^2} + \frac{\partial^3 v}{\partial x^2 \partial y} \right) \\
& + B_{22}^s \frac{\partial^3 v}{\partial y^3} - D_{11}^s \frac{\partial^4 w_b}{\partial x^4} - 2(D_{12}^s + 2D_{66}^s) \frac{\partial^4 w_b}{\partial x^2 \partial y^2} - D_{22}^s \frac{\partial^4 w_b}{\partial y^4} \\
& - H_{11}^s \frac{\partial^4 w_s}{\partial x^4} - 2(H_{12}^s + 2H_{66}^s) \frac{\partial^4 w_s}{\partial x^2 \partial y^2} - H_{22}^s \frac{\partial^4 w_s}{\partial y^4} \\
& + A_{55}^s \frac{\partial^2 w_s}{\partial x^2} + A_{44}^s \frac{\partial^2 w_s}{\partial y^2} - k_w (w_b + w_s) \\
& + k_p \left(\frac{\partial^2 (w_b + w_s)}{\partial x^2} + \frac{\partial^2 (w_b + w_s)}{\partial y^2} \right) \\
& - c_d \frac{\partial (w_b + w_s)}{\partial t} - I_0 \frac{\partial^2 (w_b + w_s)}{\partial t^2} \\
& - J_1 \left(\frac{\partial^3 u}{\partial x \partial t^2} + \frac{\partial^3 v}{\partial y \partial t^2} \right) + J_2 \left(\frac{\partial^4 w_b}{\partial x^2 \partial t^2} + \frac{\partial^4 w_b}{\partial y^2 \partial t^2} \right) \\
& + K_2 \left(\frac{\partial^4 w_s}{\partial x^2 \partial t^2} + \frac{\partial^4 w_s}{\partial y^2 \partial t^2} \right) = 0
\end{aligned} \tag{35}$$

3 Solution procedure

In this part, Galerkin's method is utilized in order to achieve the natural frequency of the porous metal foam plates. According to this analytical method, the displacement field can be expressed in the following form [19]:

$$\begin{aligned}
u &= \sum_{m=1}^{\infty} \sum_{n=1}^{\infty} U_{mn} \frac{\partial X_m(x)}{\partial x} Y_n(y) e^{i\omega_n t}, \\
v &= \sum_{m=1}^{\infty} \sum_{n=1}^{\infty} V_{mn} X_m(x) \frac{\partial Y_n(y)}{\partial y} e^{i\omega_n t}, \\
w_b &= \sum_{m=1}^{\infty} \sum_{n=1}^{\infty} W_{bmn} X_m(x) Y_n(y) e^{i\omega_n t}, \\
w_s &= \sum_{m=1}^{\infty} \sum_{n=1}^{\infty} W_{smn} X_m(x) Y_n(y) e^{i\omega_n t}
\end{aligned} \tag{36}$$

in which U_{mn} , V_{mn} , W_{bmn} and W_{smn} are unknown coefficients. Moreover, X_m and Y_n are trigonometric functions in terms of x and y , respectively; these functions are majorly presented to satisfy the BCs on edges of the plate. The preliminary assumptions for simply support and clamped BCs are:

- Simply supported–simply supported (S–S):

$$w_b = w_s = N_x = M_x = 0 \text{ at } x = 0, a$$

$$w_b = w_s = N_y = M_y = 0 \text{ at } y = 0, b$$

- Clamped–clamped (C–C):

$$u = v = w_b = w_s = 0 \text{ at } x = 0, a \text{ and } y = 0, b$$

Now, inserting Eq. (36) in Eqs. (32)–(35) and integrating over the cross-sectional area of the plate results in the following eigenvalue problem:

$$[K]\Delta + [C]\omega_n \Delta - [M]\omega_n^2 \Delta = 0 \tag{37}$$

where Δ is a column vector including unknown coefficients. Also, K , C and M denote stiffness, damping and mass matrices, respectively. The corresponding arrays of such matrices can be found looking for “Appendix” at the end. Here, X_m and Y_n functions corresponding with SSSS and CCCC supports can be assumed to be as [9]:

$$\begin{aligned}
\text{SSSS: } X_m &= \sin\left(\frac{m\pi x}{a}\right), \quad Y_n = \sin\left(\frac{n\pi y}{b}\right) \\
\text{CCCC: } X_m &= \sin^2\left(\frac{m\pi x}{a}\right), \quad Y_n = \sin^2\left(\frac{n\pi y}{b}\right)
\end{aligned} \tag{38}$$

4 Numerical results and discussion

The present section is dedicated to present a group of numerical illustrations for the purpose of highlighting the effects of different variants on the natural frequency of the porous rectangular plates. In this study, the material properties of the metal foam are assumed to be $E_1 = 200$ GPa, $\rho_1 = 7850$ kg/m³, $\nu = 0.33$. Also, the plate's thickness is considered to be $h = 5$ mm in all of the diagrams. Here, the dimensionless form of the natural frequency and

Table 1 Comparison of the first dimensionless frequency of FG square plates

<i>ah</i>		Power law index, <i>p</i>					
		0	0.5	1	2	5	10
5	Thai et al. [23]	5.2813	4.5180	4.0781	3.6805	3.3938	3.2514
	Present	5.2813	4.5073	4.0762	3.6783	3.3926	3.2515
10	Thai et al. [23]	5.7694	4.9014	4.4192	4.0090	3.7682	3.6368
	Present	5.7694	4.8899	4.4185	4.0082	3.7678	3.6373
20	Thai et al. [23]	5.9199	5.0180	4.5228	4.1100	3.8884	3.7622
	Present	5.9198	5.0061	4.5226	4.1098	3.8883	3.7629
100	Thai et al. [23]	5.9712	5.0575	4.5579	4.1445	3.9299	3.8058
	Present	5.9711	5.0456	4.5579	4.1445	3.9300	3.8065

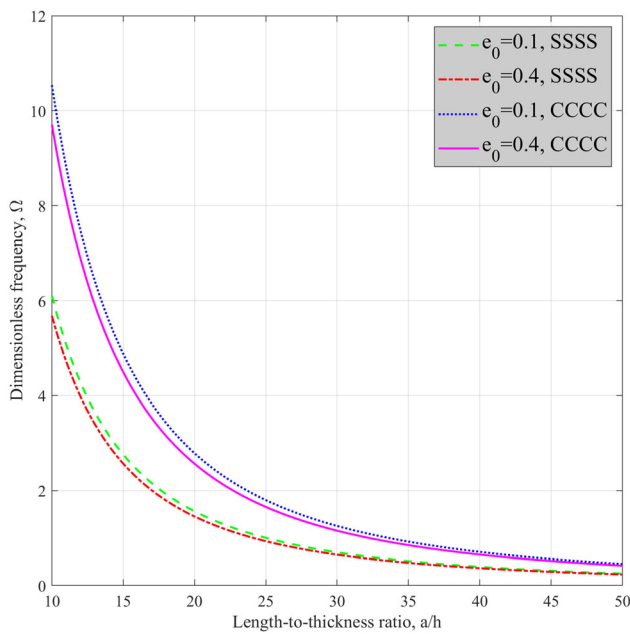


Fig. 2 Variation of the first dimensionless frequency of square porous plates versus length-to-thickness ratio for various BCs and porosity coefficients ($K_w = 20, K_p = 2, C_d = 5$)

foundation parameters will be introduced in the following for the sake of simplicity:

$$\Omega = 100 \omega h \sqrt{\rho_1/E_1}, \quad K_w = \frac{k_w a^4}{D^*}, \quad K_p = \frac{k_p a^2}{D^*}, \quad (39)$$

$$C_d = \frac{c_d a^2}{\sqrt{\rho_1 h D^*}}, \quad D^* = \frac{E_1 h^3}{12(1 - \nu^2)}$$

First of all, the validation of the introduced methodology is examined here by comparing the presented results with those reported by Thai et al. [23]. As given in Table 1, one can see a remarkable agreement between the results of our modeling and those reported by Thai et al. [23].

Figure 2 is depicted to illustrate the combined influences of BC and porosity coefficient on the frequency behaviors of metal foam porous plates. In this diagram, the variation of the first dimensionless frequency is plotted against length-to-thickness ratio for square plates. It can be

realized that the more is the length-to-thickness ratio, the smaller is the frequency which can be tolerated by the structure. The physical reason for this phenomenon is that the structure becomes stiffer once a small value is assigned to the length-to-thickness ratio and hence, the plate can provide higher frequencies. Moreover, the observations reveal that fully clamped plates are able to support greater resonance frequencies in comparison with the plates with all edges simply-supported. Also, it is evident that the frequency of the system will be decreased in the situation that the porosity coefficient is increased. Indeed, as the porosities increase in the continua, the stiffness of the plate will be lessened and due to the direct relation between the frequency and stiffness the frequency will be lessened, too.

Furthermore, the main objective of presenting Figs. 3 and 4 is to investigate how various patterns of porosity can affect the natural frequency of SSSS square metal foam porous plates as well as showing the effects of Winkler and Pasternak coefficients, respectively. It is obvious that among these three types of porosity distributions, the symmetric one can provide higher natural frequencies compared with the others followed by asymmetric and uniform. Again, it is observed that the frequency responses of the plates can be decreased whenever the porosity coefficient is added. It is worth mentioning that the effect of changing the coefficient of porosity can be better observed in uniform and asymmetric porosity distributions. In fact, the frequency change is minimum in the case of choosing a porous metal foam plate with symmetric porosity distribution. Clearly, increasing each of the Winkler and Pasternak coefficients can improve the natural frequency of the plate. However, the efficiency of these two elastic stiffnesses is not the same. In other words, in a constant value for the dimensionless stiffness, Pasternak coefficient can affect the frequency more than Winkler coefficient.

Besides, in Fig. 5, both SSSS and CCCC BCs are undertaken in order to show the variation of the dimensionless frequency versus aspect ratio for various coefficients of the viscoelastic medium. It is again shown that CCCC plates can tolerate higher natural frequencies

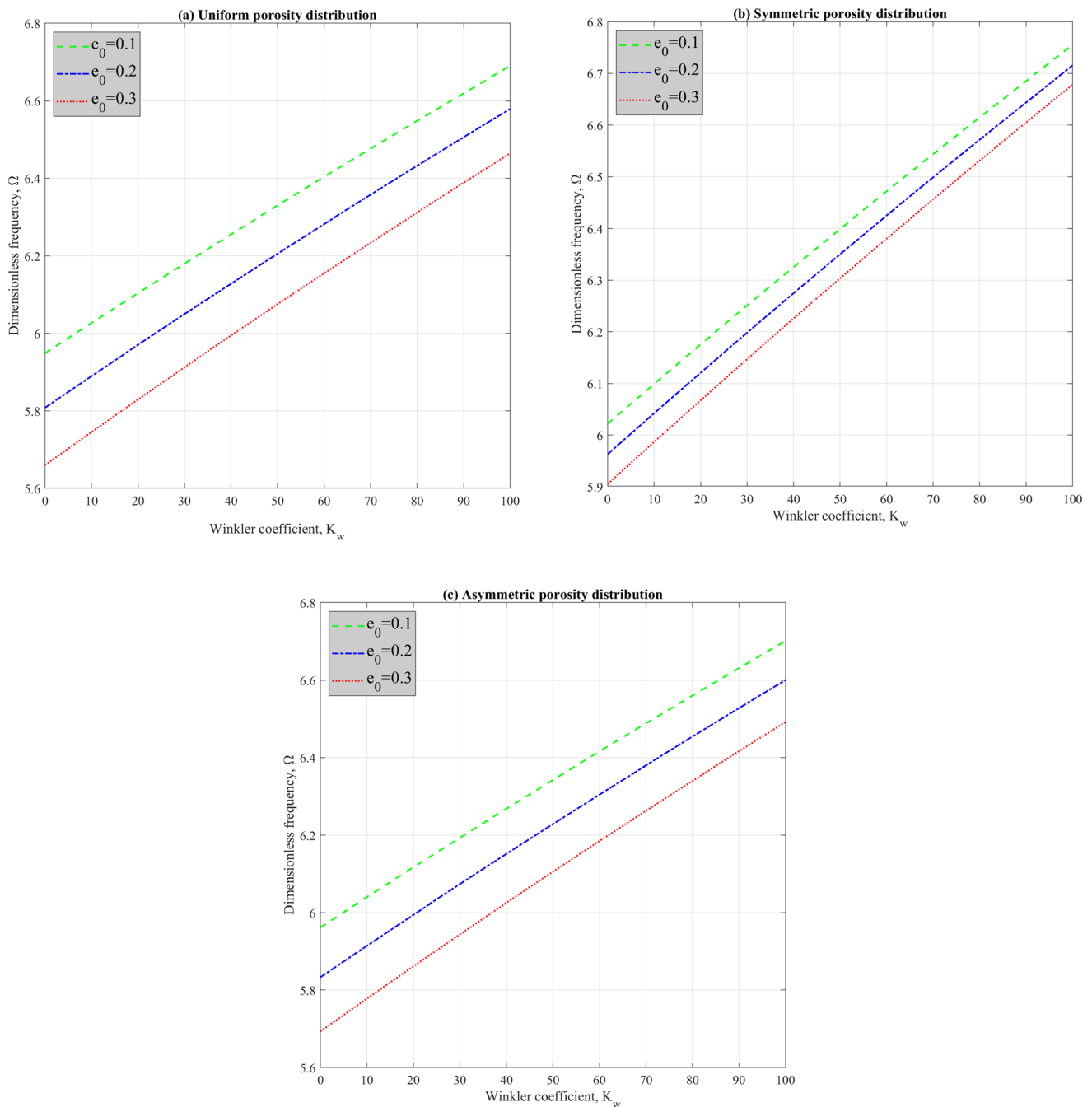


Fig. 3 Variation of the first dimensionless frequency of SSSS square porous plates against Winkler coefficient for various porosity coefficients and porosity distributions ($alh = 10$, $K_p = 2$, $C_d = 5$)

compared with SSSS ones. Also, one should pay attention that an increase in the elastic constants of the substrate, namely Winkler and Pasternak coefficients, can aggrandize the frequency, whereas a similar increase in the magnitude of damping coefficient results in reaching lower frequencies.

Figure 6 is devoted to show the variation of the dimensionless frequency versus damping coefficient of the viscoelastic medium for various porosity distributions of a SSSS porous metal foam plate. As shown in this figure,

adding the damping coefficient can lessen the dimensionless frequency in a continuous manner. This decreasing trend will finally result in diminishing the natural frequency. Also, as well as former illustrations, herein, the symmetric porosity distribution possesses highest frequency followed by asymmetric and uniform distributions.

At the end, influences of a group of variants are going to be reviewed in Fig. 7 to highlight their effects on the variation of the dimensionless natural frequency of SSSS

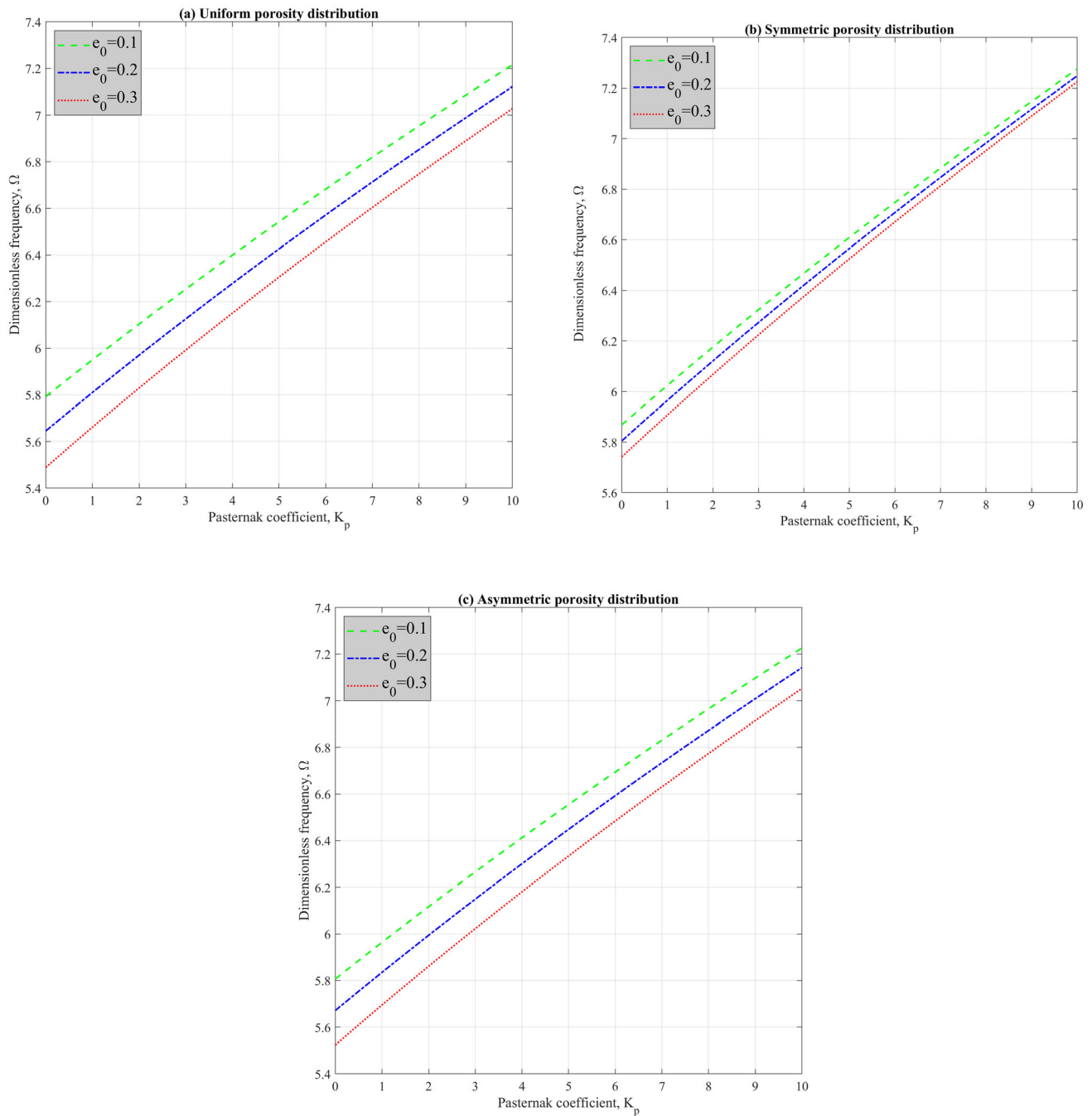


Fig. 4 Variation of the first dimensionless frequency of SSSS square porous plates against Pasternak coefficient for various porosity coefficients and porosity distributions ($a/h = 10$, $K_w = 20$, $C_d = 5$)

porous metal foam plates. As same as Fig. 6, the frequency will be damped gradually as the damping coefficient of the viscoelastic foundation is increased. Also, once again it can be shown that structures that are rested on elastic springs are better candidates for the situations which huge dynamic frequencies are seemed to be endured by the structure. Moreover, it can be figured out that the dimensionless frequency of the plate will be decreased, while the porosity coefficient is risen.

5 Conclusions

This manuscript was arranged to probe the vibrational characteristics of metal foam plates rested on a viscoelastic foundation with respect to the influences of different porosity distributions. The motion equations were obtained via the Hamilton’s principle combined with a refined higher-order shear deformation plate theory. Finally, the equations were solved according to the Galerkin’s method.

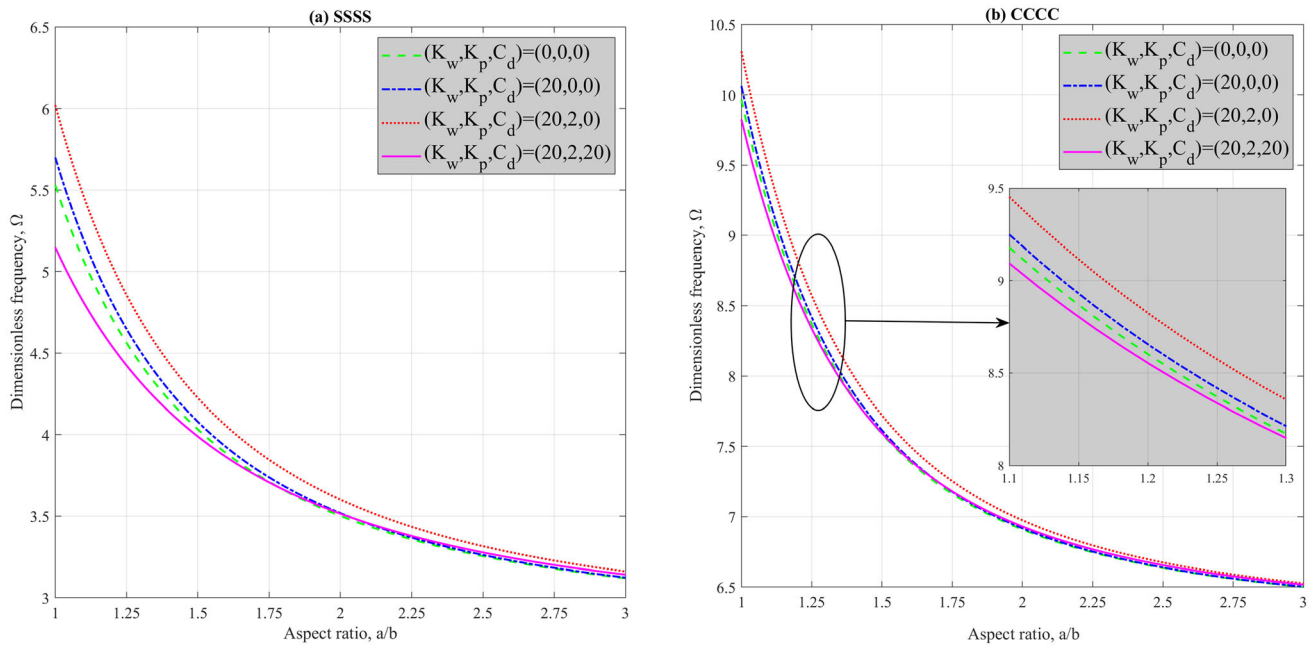


Fig. 5 Variation of the first dimensionless frequency of the rectangular porous plates versus aspect ratio for various foundation parameters and BCs for uniformly porous metal foams ($b/h = 10, e_0 = 0.2$)

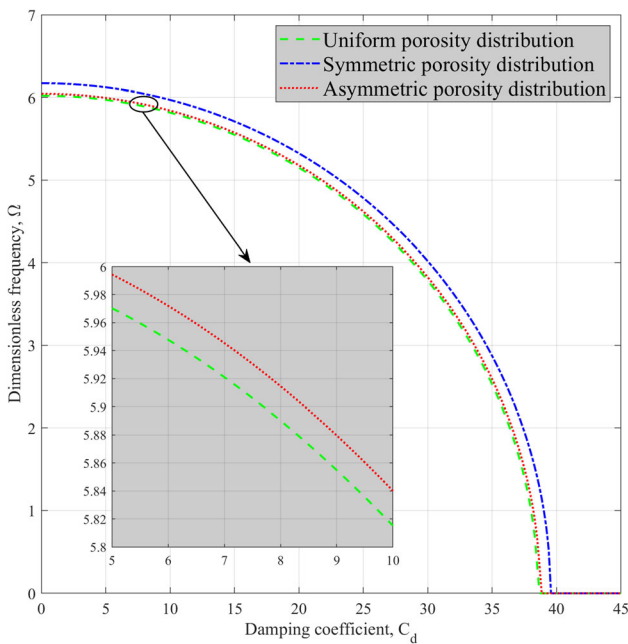


Fig. 6 Variation of the first dimensionless frequency of SSSS square porous plates versus damping coefficient for various porosity distributions ($a/h = 10, K_w = 20, K_p = 2, e_0 = 0.2$)

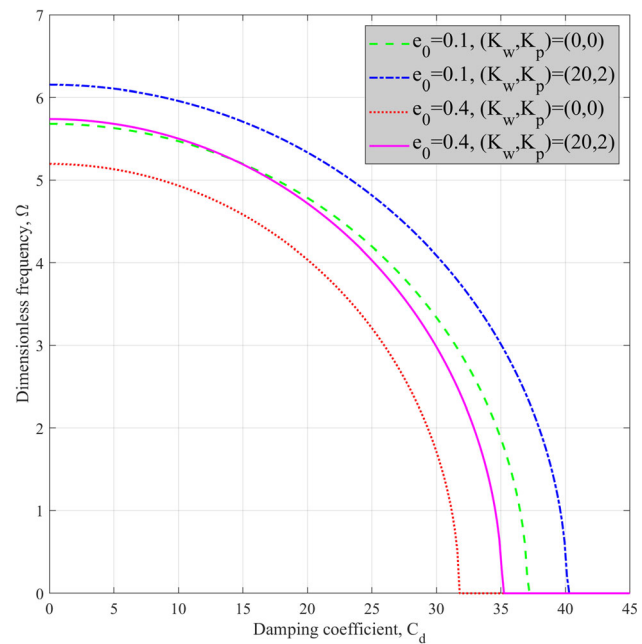


Fig. 7 Variation of the first dimensionless frequency of SSSS square porous plates versus damping coefficient for various porosity, Winkler and Pasternak coefficients for the uniformly porous metal foams ($a/h = 10$)

Herein, the most crucial highlights are presented in the following:

- The dimensionless frequency becomes smaller, while the porosity coefficient grows.
- Among three types of porosity distributions, symmetric one provides highest frequency responses.

- The CCCC plates are able to support higher frequency ranges in comparison with the SSSS ones.
- The frequency can be increased by employing higher elastic foundation parameters.

- The frequency can be damped, while the damping coefficient of the viscoelastic medium is added.
- Both length-to-thickness and aspect ratios are able to lessen the dimensionless frequency whenever they are added.

Appendix

The components of stiffness and mass matrices can be calculated by:

$$\begin{aligned}
 k_{11} &= A_{11} \int_0^b \int_0^a \frac{\partial X_m(x)}{\partial x} Y_n(y) \frac{\partial^3 X_m(x)}{\partial x^3} Y_n(y) dx dy \\
 &\quad + A_{66} \int_0^b \int_0^a \frac{\partial X_m(x)}{\partial x} Y_n(y) \frac{\partial X_m(x)}{\partial x} \frac{\partial^2 Y_n(y)}{\partial y^2} dx dy, \\
 k_{12} &= (A_{12} + A_{66}) \int_0^b \int_0^a \frac{\partial X_m(x)}{\partial x} Y_n(y) \frac{\partial X_m(x)}{\partial x} \frac{\partial^2 Y_n(y)}{\partial y^2} dx dy, \\
 k_{13} &= -B_{11} \int_0^b \int_0^a \frac{\partial X_m(x)}{\partial x} Y_n(y) \frac{\partial^3 X_m(x)}{\partial x^3} Y_n(y) dx dy \\
 &\quad - (B_{12} + 2B_{66}) \int_0^b \int_0^a \frac{\partial X_m(x)}{\partial x} Y_n(y) \frac{\partial X_m(x)}{\partial x} \frac{\partial^2 Y_n(y)}{\partial y^2} dx dy, \\
 k_{14} &= -B_{11}^s \int_0^b \int_0^a \frac{\partial X_m(x)}{\partial x} Y_n(y) \frac{\partial^3 X_m(x)}{\partial x^3} Y_n(y) dx dy \\
 &\quad - (B_{12}^s + 2B_{66}^s) \int_0^b \int_0^a \frac{\partial X_m(x)}{\partial x} Y_n(y) \frac{\partial X_m(x)}{\partial x} \frac{\partial^2 Y_n(y)}{\partial y^2} dx dy, \\
 k_{21} &= (A_{12} + A_{66}) \int_0^b \int_0^a X_m(x) \frac{\partial Y_n(y)}{\partial y} \frac{\partial^2 X_m(x)}{\partial x^2} \frac{\partial Y_n(y)}{\partial y} dx dy, \quad 22 \\
 &\quad + A_{22} \int_0^b \int_0^a X_m(x) \frac{\partial Y_n(y)}{\partial y} X_m(x) \frac{\partial^3 Y_n(y)}{\partial y^3} dx dy, \\
 k_{23} &= -(B_{12} + 2B_{66}) \int_0^b \int_0^a X_m(x) \frac{\partial Y_n(y)}{\partial y} \frac{\partial^2 X_m(x)}{\partial x^2} \frac{\partial Y_n(y)}{\partial y} dx dy \\
 &\quad - B_{22} \int_0^b \int_0^a X_m(x) \frac{\partial Y_n(y)}{\partial y} X_m(x) \frac{\partial^3 Y_n(y)}{\partial y^3} dx dy, \\
 k_{24} &= -(B_{12}^s + 2B_{66}^s) \int_0^b \int_0^a X_m(x) \frac{\partial Y_n(y)}{\partial y} \frac{\partial^2 X_m(x)}{\partial x^2} \frac{\partial Y_n(y)}{\partial y} dx dy \\
 &\quad - B_{22}^s \int_0^b \int_0^a X_m(x) \frac{\partial Y_n(y)}{\partial y} X_m(x) \frac{\partial^3 Y_n(y)}{\partial y^3} dx dy, \\
 k_{31} &= B_{11} \int_0^b \int_0^a X_m(x) Y_n(y) \frac{\partial^4 X_m(x)}{\partial x^4} Y_n(y) dx dy + (B_{12} + 2B_{66}) \\
 &\quad \times \int_0^b \int_0^a X_m(x) Y_n(y) \frac{\partial^2 X_m(x)}{\partial x^2} \frac{\partial^2 Y_n(y)}{\partial y^2} dx dy,
 \end{aligned}$$

$$\begin{aligned}
 k_{32} &= (B_{12} + 2B_{66}) \int_0^b \int_0^a X_m(x) Y_n(y) \frac{\partial^2 X_m(x)}{\partial x^2} \frac{\partial^2 Y_n(y)}{\partial y^2} dx dy \\
 &\quad + B_{22} \int_0^b \int_0^a X_m(x) Y_n(y) X_m(x) \frac{\partial^4 Y_n(y)}{\partial y^4} dx dy,
 \end{aligned}$$

$$\begin{aligned}
 k_{33} &= -D_{11} \int_0^b \int_0^a X_m(x) Y_n(y) \frac{\partial^4 X_m(x)}{\partial x^4} Y_n(y) dx dy - 2(D_{12} + 2D_{66}) \\
 &\quad \times \int_0^b \int_0^a X_m(x) Y_n(y) \frac{\partial^2 X_m(x)}{\partial x^2} \frac{\partial^2 Y_n(y)}{\partial y^2} dx dy \\
 &\quad - D_{22} \int_0^b \int_0^a X_m(x) Y_n(y) X_m(x) \frac{\partial^4 Y_n(y)}{\partial y^4} dx dy \\
 &\quad - k_w \int_0^b \int_0^a X_m(x) Y_n(y) X_m(x) Y_n(y) dx dy \\
 &\quad + k_p \left(\int_0^b \int_0^a X_m(x) Y_n(y) \frac{\partial^2 X_m(x)}{\partial x^2} Y_n(y) dx dy \right. \\
 &\quad \left. + \int_0^b \int_0^a X_m(x) Y_n(y) X_m(x) \frac{\partial^2 Y_n(y)}{\partial y^2} dx dy \right),
 \end{aligned}$$

$$\begin{aligned}
 k_{34} &= -D_{11}^s \int_0^b \int_0^a X_m(x) Y_n(y) \frac{\partial^4 X_m(x)}{\partial x^4} Y_n(y) dx dy \\
 &\quad - 2(D_{12}^s + 2D_{66}^s) \int_0^b \int_0^a X_m(x) Y_n(y) \frac{\partial^2 X_m(x)}{\partial x^2} \frac{\partial^2 Y_n(y)}{\partial y^2} dx dy \\
 &\quad - D_{22}^s \int_0^b \int_0^a X_m(x) Y_n(y) X_m(x) \frac{\partial^4 Y_n(y)}{\partial y^4} dx dy \\
 &\quad - k_w \int_0^b \int_0^a X_m(x) Y_n(y) X_m(x) Y_n(y) dx dy \\
 &\quad + k_p \left(\int_0^b \int_0^a X_m(x) Y_n(y) \frac{\partial^2 X_m(x)}{\partial x^2} Y_n(y) dx dy \right. \\
 &\quad \left. + \int_0^b \int_0^a X_m(x) Y_n(y) X_m(x) \frac{\partial^2 Y_n(y)}{\partial y^2} dx dy \right), \quad 41 \\
 &\quad + (B_{12}^s + 2B_{66}^s) \int_0^b \int_0^a \frac{\partial^2 X_m(x)}{\partial x^2} Y_n(y) X_m(x) \frac{\partial^2 Y_n(y)}{\partial y^2} dx dy,
 \end{aligned}$$

$$\begin{aligned}
 k_{42} &= (B_{12}^s + 2B_{66}^s) \int_0^b \int_0^a X_m(x) Y_n(y) \frac{\partial^2 X_m(x)}{\partial x^2} \frac{\partial^2 Y_n(y)}{\partial y^2} dx dy \\
 &\quad + B_{22}^s \int_0^b \int_0^a X_m(x) Y_n(y) X_m(x) \frac{\partial^4 Y_n(y)}{\partial y^4} dx dy,
 \end{aligned}$$

$$k_{43} = -D_{11}^s \int_0^b \int_0^a X_m(x) Y_n(y) \frac{\partial^4 X_m(x)}{\partial x^4} Y_n(y) dx dy$$

$$\begin{aligned}
 & - 2(D_{12}^s + 2D_{66}^s) \int_0^b \int_0^a X_m(x) Y_n(y) \frac{\partial^2 X_m(x)}{\partial x^2} \frac{\partial^2 Y_n(y)}{\partial y^2} dx dy \\
 & - D_{22}^s \int_0^b \int_0^a X_m(x) Y_n(y) X_m(x) \frac{\partial^4 Y_n(y)}{\partial y^4} dx dy \\
 & - k_w \int_0^b \int_0^a X_m(x) Y_n(y) X_m(x) Y_n(y) dx dy \\
 & + k_p \left(\int_0^b \int_0^a X_m(x) Y_n(y) \frac{\partial^2 X_m(x)}{\partial x^2} Y_n(y) dx dy \right. \\
 & \left. + \int_0^b \int_0^a X_m(x) Y_n(y) X_m(x) \frac{\partial^2 Y_n(y)}{\partial y^2} dx dy \right), \\
 k_{44} = & -H_{11}^s \int_0^b \int_0^a X_m(x) Y_n(y) \frac{\partial^4 X_m(x)}{\partial x^4} Y_n(y) dx dy \\
 & - 2(H_{12}^s + 2H_{66}^s) \int_0^b \int_0^a X_m(x) Y_n(y) \frac{\partial^2 X_m(x)}{\partial x^2} \frac{\partial^2 Y_n(y)}{\partial y^2} dx dy \\
 & - H_{22}^s \int_0^b \int_0^a X_m(x) Y_n(y) X_m(x) \frac{\partial^4 Y_n(y)}{\partial y^4} dx dy \\
 & + A_{44}^s \int_0^b \int_0^a X_m(x) Y_n(y) \frac{\partial^2 X_m(x)}{\partial x^2} Y_n(y) dx dy \\
 & + A_{44}^s \int_0^b \int_0^a X_m(x) Y_n(y) X_m(x) \frac{\partial^2 Y_n(y)}{\partial y^2} dx dy \\
 & - k_w \int_0^b \int_0^a X_m(x) Y_n(y) X_m(x) Y_n(y) dx dy \\
 & + k_p \left(\int_0^b \int_0^a X_m(x) Y_n(y) \frac{\partial^2 X_m(x)}{\partial x^2} Y_n(y) dx dy \right. \\
 & \left. + \int_0^b \int_0^a X_m(x) Y_n(y) X_m(x) \frac{\partial^2 Y_n(y)}{\partial y^2} dx dy \right)
 \end{aligned}$$

and

$$\begin{aligned}
 m_{11} = & -I_0 \int_0^b \int_0^a \frac{\partial X_m(x)}{\partial x} Y_n(y) \frac{\partial X_m(x)}{\partial x} Y_n(y) dx dy, \\
 m_{13} = & I_1 \int_0^b \int_0^a \frac{\partial X_m(x)}{\partial x} Y_n(y) \frac{\partial X_m(x)}{\partial x} Y_n(y) dx dy, \\
 m_{14} = & J_1 \int_0^b \int_0^a \frac{\partial X_m(x)}{\partial x} Y_n(y) \frac{\partial X_m(x)}{\partial x} Y_n(y) dx dy, \\
 m_{22} = & -I_0 \int_0^b \int_0^a X_m(x) \frac{\partial Y_n(y)}{\partial y} X_m(x) \frac{\partial Y_n(y)}{\partial y} dx dy, \\
 m_{23} = & I_1 \int_0^b \int_0^a X_m(x) \frac{\partial Y_n(y)}{\partial y} X_m(x) \frac{\partial Y_n(y)}{\partial y} dx dy, \\
 m_{24} = & J_1 \int_0^b \int_0^a X_m(x) \frac{\partial Y_n(y)}{\partial y} X_m(x) \frac{\partial Y_n(y)}{\partial y} dx dy, \\
 m_{31} = & -I_1 \int_0^b \int_0^a X_m(x) Y_n(y) \frac{\partial^2 X_m(x)}{\partial x^2} Y_n(y) dx dy, \\
 m_{32} = & -I_1 \int_0^b \int_0^a X_m(x) Y_n(y) X_m(x) \frac{\partial^2 Y_n(y)}{\partial y^2} dx dy, \\
 m_{33} = & -I_0 \int_0^b \int_0^a X_m(x) Y_n(y) X_m(x) Y_n(y) dx dy \\
 & + I_2 \left(\int_0^b \int_0^a X_m(x) Y_n(y) \frac{\partial^2 X_m(x)}{\partial x^2} Y_n(y) dx dy + \int_0^b \int_0^a X_m(x) Y_n(y) X_m(x) \frac{\partial^2 Y_n(y)}{\partial y^2} dx dy \right), \\
 m_{34} = & -I_0 \int_0^b \int_0^a X_m(x) Y_n(y) X_m(x) Y_n(y) dx dy \\
 & + J_2 \left(\int_0^b \int_0^a X_m(x) Y_n(y) \frac{\partial^2 X_m(x)}{\partial x^2} Y_n(y) dx dy + \int_0^b \int_0^a X_m(x) Y_n(y) X_m(x) \frac{\partial^2 Y_n(y)}{\partial y^2} dx dy \right), \\
 m_{41} = & -J_1 \int_0^b \int_0^a \frac{\partial^2 X_m(x)}{\partial x^2} Y_n(y) X_m(x) Y_n(y) dx dy, \\
 m_{42} = & -J_1 \int_0^b \int_0^a X_m(x) Y_n(y) X_m(x) \frac{\partial^2 Y_n(y)}{\partial y^2} dx dy, \\
 m_{43} = & -I_0 \int_0^b \int_0^a X_m(x) Y_n(y) X_m(x) Y_n(y) dx dy \\
 & + J_2 \left(\int_0^b \int_0^a X_m(x) Y_n(y) \frac{\partial^2 X_m(x)}{\partial x^2} Y_n(y) dx dy + \int_0^b \int_0^a X_m(x) Y_n(y) X_m(x) \frac{\partial^2 Y_n(y)}{\partial y^2} dx dy \right), \\
 m_{44} = & -I_0 \int_0^b \int_0^a X_m(x) Y_n(y) X_m(x) Y_n(y) dx dy \\
 & + K_2 \left(\int_0^b \int_0^a X_m(x) Y_n(y) \frac{\partial^2 X_m(x)}{\partial x^2} Y_n(y) dx dy + \int_0^b \int_0^a X_m(x) Y_n(y) X_m(x) \frac{\partial^2 Y_n(y)}{\partial y^2} dx dy \right)
 \end{aligned} \tag{40}$$

and

$$\begin{aligned}
 C_{33} = & C_{34} = C_{43} = C_{44} \\
 = & -ic_d \int_0^b \int_0^a X_m(x) Y_n(y) X_m(x) Y_n(y) dx dy
 \end{aligned} \tag{42}$$

References

- Jabbari M, Mojahedin A, Khorshidvand AR, Eslami MR (2013) Buckling analysis of a functionally graded thin circular plate made of saturated porous materials. *J Eng Mech* 140(2):287–295
- Jabbari M, Hashemitaheeri M, Mojahedin A, Eslami MR (2014) Thermal buckling analysis of functionally graded thin circular plate made of saturated porous materials. *J Therm Stresses* 37(2):202–220
- Wattanasakulpong N, Ungbhakorn V (2014) Linear and nonlinear vibration analysis of elastically restrained ends FGM beams with porosities. *Aerosp Sci Technol* 32(1):111–120
- Chen D, Yang J, Kitipornchai S (2015) Elastic buckling and static bending of shear deformable functionally graded porous beam. *Compos Struct* 133:54–61
- Chen D, Yang J, Kitipornchai S (2016) Free and forced vibrations of shear deformable functionally graded porous beams. *Int J Mech Sci* 108:14–22
- Chen D, Kitipornchai S, Yang J (2016) Nonlinear free vibration of shear deformable sandwich beam with a functionally graded porous core. *Thin-Walled Struct* 107:39–48
- Rezaei AS, Saidi AR (2016) Application of Carrera Unified Formulation to study the effect of porosity on natural frequencies of thick porous–cellular plates. *Compos B Eng* 91:361–370. <https://doi.org/10.1016/B978-0-7506-8560-3.X0001-1>
- Atmane HA, Tounsi A, Bernard F (2017) Effect of thickness stretching and porosity on mechanical response of a functionally graded beams resting on elastic foundations. *Int J Mech Mater Des* 13(1):71–84
- Barati MR, Zenkour AM (2018) Electro-thermoelastic vibration of plates made of porous functionally graded piezoelectric materials under various boundary conditions. *J Vib Control* 24(10):1910–1926
- Toan Thang P, Nguyen-Thoi T, Lee J (2018) Mechanical stability of metal foam cylindrical shells with various porosity distributions. *Mech Adv Mater Struct* 27(4):1–9
- Vaidya UK, Pillay S, Bartus S, Ulven CA, Grow DT, Mathew B (2006) Impact and post-impact vibration response of protective metal foam composite sandwich plates. *Mater Sci Eng, A* 428(1–2):59–66
- Debowski D, Magnucki K, Malinowski M (2010) Dynamic stability of a metal foam rectangular plate. *Steel Compos Struct* 10(2):151–168
- Magnucka-Blandzi E (2011) Mathematical modelling of a rectangular sandwich plate with a metal foam core. *J Theor Appl Mech* 49(2):439–455
- Qin QH, Wang TJ (2012) Plastic analysis of metal foam core sandwich beam transversely loaded by a flat punch: combined local denting and overall deformation. *J Appl Mech* 79(4):041010
- Jasion P, Magnucka-Blandzi E, Szyc W, Magnucki K (2012) Global and local buckling of sandwich circular and beam-rectangular plates with metal foam core. *Thin-Walled Struct* 61:154–161
- Qin Q, Zheng X, Zhang J, Yuan C, Wang TJ (2018) Dynamic response of square sandwich plates with a metal foam core subjected to low-velocity impact. *Int J Impact Eng* 111:222–235
- Ebrahimi F, Dabbagh A, Rastgoo A (2019) Vibration analysis of porous metal foam shells rested on an elastic substrate. *J Strain Anal Eng Des* 54(3):199–208. <https://doi.org/10.1177/0309324719852555>
- Ebrahimi F, Dabbagh A (2019) An analytical solution for static stability of multi-scale hybrid nanocomposite plates. *Eng Comput*. <https://doi.org/10.1007/s00366-019-00840-y>
- Ebrahimi F, Dabbagh A, Rastgoo A (2019) Free vibration analysis of multi-scale hybrid nanocomposite plates with agglomerated nanoparticles. *Mech Based Des Struct Mach*. <https://doi.org/10.1080/15397734.2019.1692665>
- Ebrahimi F, Dabbagh A (2020) *Mechanics of nanocomposites: homogenization and analysis*, 1st ed. CRC Press, Boca Raton. <https://doi.org/10.1201/9780429316791>
- Zaoui FZ, Ouinas D, Tounsi A (2019) New 2D and quasi-3D shear deformation theories for free vibration of functionally graded plates on elastic foundations. *Compos B Eng* 159:231–247. <https://doi.org/10.1016/j.compositesb.2018.09.051>
- Lai WM, Rubin DH, Krempl E, Rubin D (2009) *Introduction to continuum mechanics*, 4th edn. Butterworth-Heinemann, Oxford
- Thai H-T, Park T, Choi D-H (2013) An efficient shear deformation theory for vibration of functionally graded plates. *Arch Appl Mech* 83(1):137–149

Publisher's Note Springer Nature remains neutral with regard to jurisdictional claims in published maps and institutional affiliations.